José A. Covas[1], Sidonie F. Costa[2], Fernando M. Duarte[1]

STUDYING THE COOLING STAGE IN FUSED FILAMENT FABRICATION

Abstract: *Fused Filament Fabrication (FFF) is one of the available techniques that is capable of producing parts by additive manufacturing, i.e., by depositing thin filaments of thermoplastic polymers or composites onto a support as a vertical series of horizontal 2D slices of a 3D part. This chapter approaches FFF from a phenomenological point of view, and then focus on the deposition and cooling stage. A code capable of predicting the evolution of temperature during deposition and until cooling is completed, as well as of the final bonding between filaments is presented. The tool is then used to enlighten the effect of major processing parameters on the quality of parts.*

Keywords: *additive manufacturing, fused filament fabrication, fused deposition modelling, build orientation, filament bonding*

1. Introduction

Additive Manufacturing (AM) is a group of technologies that produces three-dimensional physical objects by gradually adding material, without the use of a mould. Since the 1980s, AM evolved from a niche method for rapid prototyping to a competitive manufacturing route, with potential substantial societal impact on various sectors such as healthcare, transportation, aerospace, electronics and construction [1]. Nevertheless, despite of the diversity of AM techniques, only a few seem to meet the practical requirements of industrial manufacturing of small series. This is the case of fused filament fabrication techniques (FFF) [2].

FFF use continuous thin filaments of thermoplastic polymers or composites that are deposited onto a support as a vertical series of horizontal 2D slices of a 3D part, which can exhibit significant geometrical complexity (see Figure 1). FFF comprise Free Form Extrusion (FFE) and the trademarked Fused Deposition Modeling (FDM). The first uses an extruder to produce the filament, whereas the second melts and extrudes a previously extruded larger filament (standard filaments have diameters of 1.75mm and 3mm). Figure 1 presents an example of a printed part, in this case a gear made of Polyether ether ketone (PEEK) (light colour) and electrically conductive PEEK (dark colour). The device was used to assess the 3D printing ability of

[1] *University of Minho, Institute for Polymers and Composites and Department of Polymer Engineering, Campus Azurém, 4804-533 Guimarães, Portugal, jcovas@dep.uminho.pt; fduarte@dep.uminho.p*

[2] *Center for Research and Innovation in Business Sciences and Information Systems (CIICESI), Porto Polytechnic Institute, Felgueiras, Portugal, sfc@estg.ipp.pt*

materials to be used by the European Space Agency to manufacture parts for satellites and other space applications [3].

This chapter approaches FFF from a phenomenological point of view, and then focus on the important deposition and cooling stage. A code to predict the evolution of temperature during deposition and until cooling is completed, as well as the resulting quality of the bonding between filaments is presented. The code is then used to study the effect of major processing parameters on the quality of the printed parts.

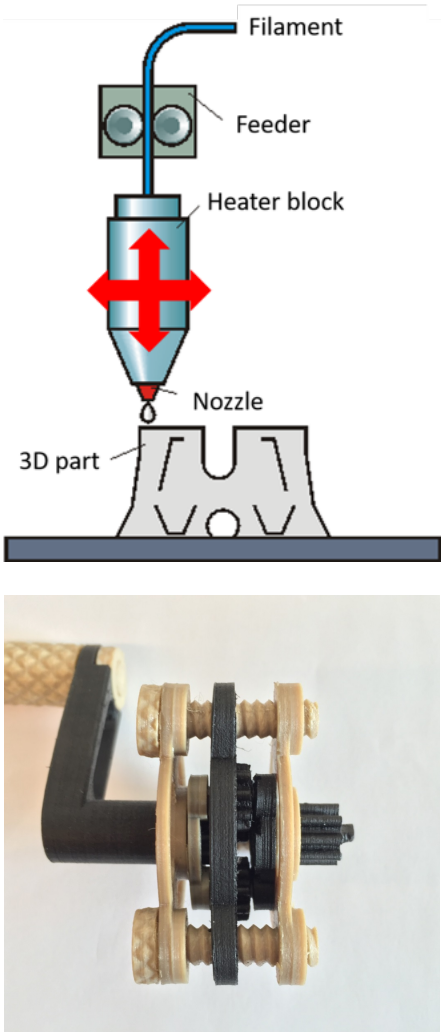

Fig. 1 Fused Filament Fabrication. Concept (top); example of a printed part made of PEEK (light colour) and electrically conductive PEEK (dark colour)(bottom).

2. Process stages

From a phenomenological point of view, FFF encompasses four main stages (see Figure 2). The first consists in feeding the filament (usually by means of a pair of counter-rotating rollers), which is then forced into the liquefier where it melts and is subsequently extruded through a nozzle (second stage). Since the filament is subjected to compression, it could eventually buckle. This led to a few technological improvements, such as using a filament guiding tube and a heat break (not represented). Flow in the liquefier is governed by the rheological properties of the melt. In the third stage, the viscoelastic melt simultaneously swells and is stretched axially by the movement of the printing head (because the velocity of the latter is usually higher than the linear velocity of the extrudate). Again, melt rheology is a determining factor.

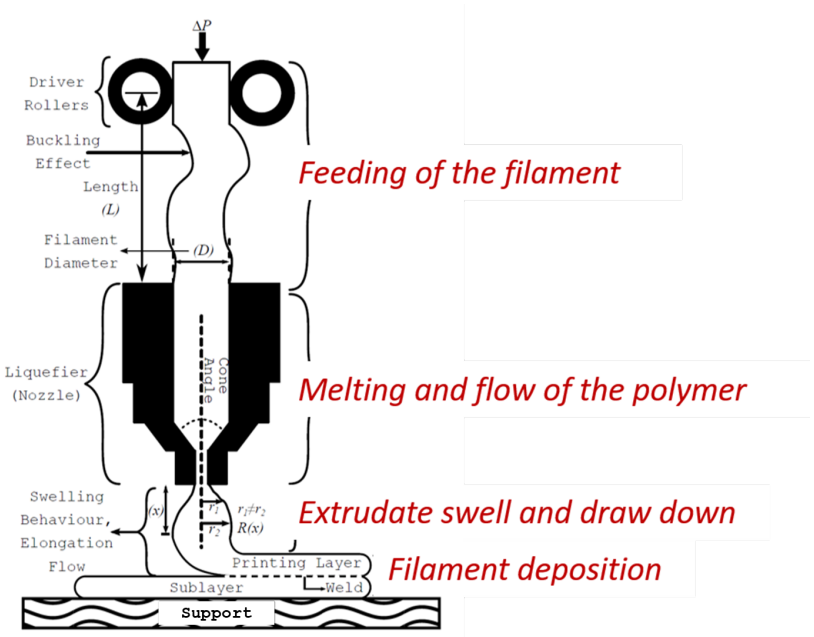

Fig.2 Main Stages of Fused Deposition Modeling

Figure 3 plots the viscosity curves (variation of viscosity with frequency) for a wide range of available commercial materials used in FFF. At the two frequencies considered (100 and 550s^{-1}), which are typically attained during printing with smaller and larger diameter filaments, respectively, the range of viscosities is relatively narrow, i.e., 320-1500s^{-1} and 195-540s^{-1}, respectively. This demonstrates

that despite its apparent simplicity and flexibility, FFF requires materials with relatively specific characteristics.

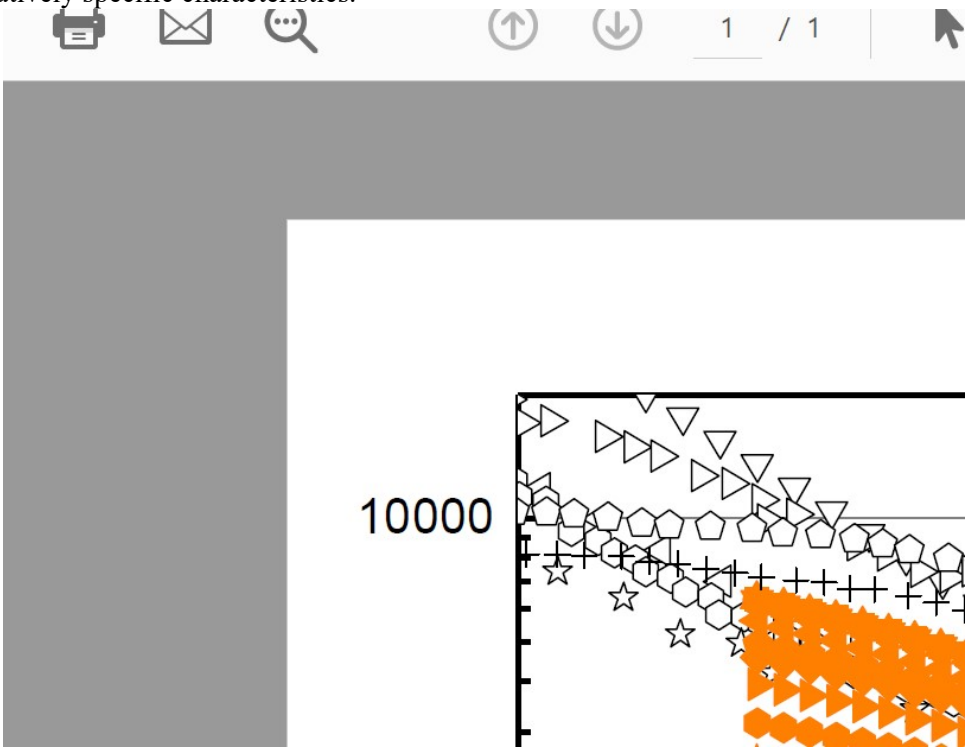

Fig. 3 Variation of viscosity with frequency for a variety of commercial materials used in FFF. The frequencies considered (100 and 550s^{-1}) are typically attained when printing with smaller and larger diameter filaments

The fourth stage consists of the actual manufacture of the part by filament deposition and cooling. As seen in Figure 4, the deposition stage involves filament deformation and bonding of contiguous filaments. Once deposited, each filament should solidify quickly to minimize the deformation due to gravity and/or the weight of the material that will be deposited above it. Conversely, it should remain sufficiently hot during enough time to ensure adequate bonding with the neighbouring filament(s). Simultaneously, differences in local shrinkage during cooling will induce the development of residual stresses which, in turn, may cause warping and eventual delamination [4]. Consequently, this stage is determinant for the quality of the final part in terms of engineering properties, surface quality and dimensional tolerances.

It has been shown experimentally that fabrication strategy, environment temperature and variations in convection determine the overall bond strength [5-7]. Figure 5 illustrates these concepts. It shows the interdependence between

temperature evolution in time and space, filament deformation and bonding between contiguous filaments, which determine the dimensional accuracy and mechanical performance, respectively. The processing parameters affecting temperature evolution are also identified.

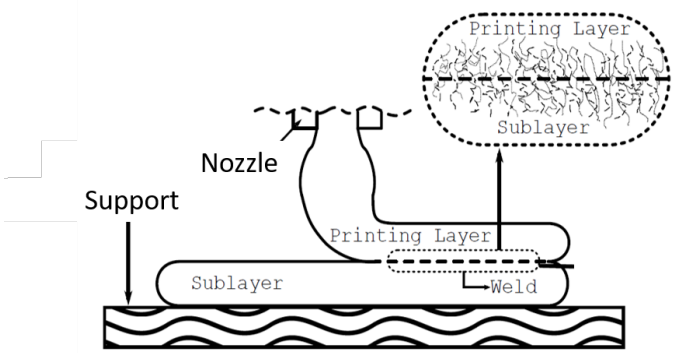

Fig 4 Filament deposition stage

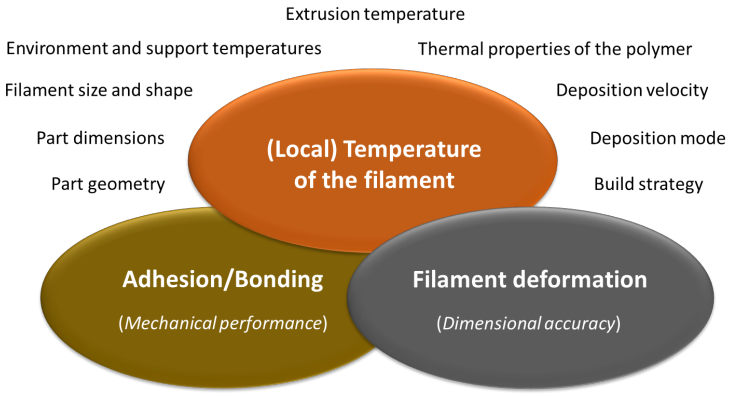

Fig 5. Effect of filament temperature on part quality and its influencing processing parameters

2. Modelling of cooling and bonding

Several authors, using different assumptions, have made predictions of filament temperature evolution during deposition. Initially, a single filament subjected to convection with the environment was considered [8, 9]. Then, cooling of a vertical filament stack was studied [10-12]. Only recently, the cooling of practical 3D parts has been tackled [13, 14].

During the deposition stage, heat exchanges by convection with the environment, by conduction between adjacent filaments and by conduction with the support are the most relevant. Moreover, the temperatures in any filament cross-section are relatively uniform [15]. Thus, modelling of heat transfer during cooling must consider the various possible contacts and corresponding heat transfer modes between any filament and its neighbors during the printing stage (see Figure 6). Filament contacts in the initial row/layer will be different from those between filaments in the remaining rows/layers, due to the presence of the support. The various heat transfer boundaries must be updated at small time increments as the deposition proceeds, being determined by the geometry of the part, build orientation and deposition sequence. Build orientation refers to the rotation of the part in the manufacturing space around the axes of the machine's coordinate system. Although it has been shown that it is a major parameter affecting the mechanical properties of parts [16], its optimization is generally performed in terms of geometrical parameters. Deposition sequence denotes the path taken by the filament during deposition, for example, unidirectional and aligned, unidirectional and skewed, or perpendicular. As with build orientation, its optimization has been mostly done with the aim of optimizing time paths, for example, by resorting to genetic algorithms [17,18]. However, the effect of deposition sequence on the mechanical properties of printed parts due to the associated changes in heat transfer has beeen recently recognized [19].

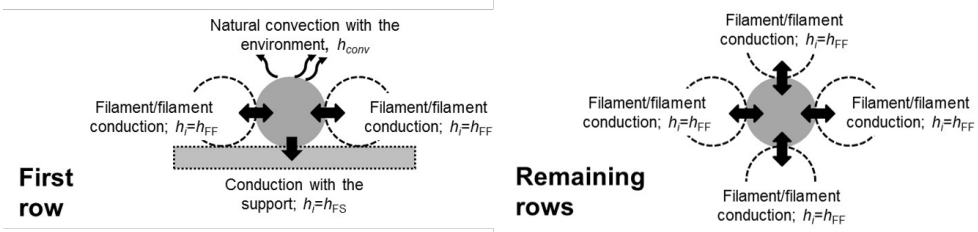

Fig. 6 Heat transfer modes in FFF for filaments in the first and remaining rows

Given the above, realistic modelling of cooling in FFF must include such aspects as thermal boundary conditions changing with time, different build orientations, and deposition sequence possibilities. The MatLab® computer code developed (Figure 7) contains an analytical solution to the transient heat conduction that is coupled to an algorithm that activates the relevant boundary conditions [13]. Also, the code incorporates a healing criterion [20], i.e., an assessment of the quality of bonding (dependent on local temperature history), that assumes non-isothermal conditions and is based on a formulation of reptation of polymer chains. The input parameters of the code include physical and thermal material properties, geometry of the part

and process parameters, such as extrusion velocity and temperature, deposition sequence, environment temperature, support temperature and filament dimensions.

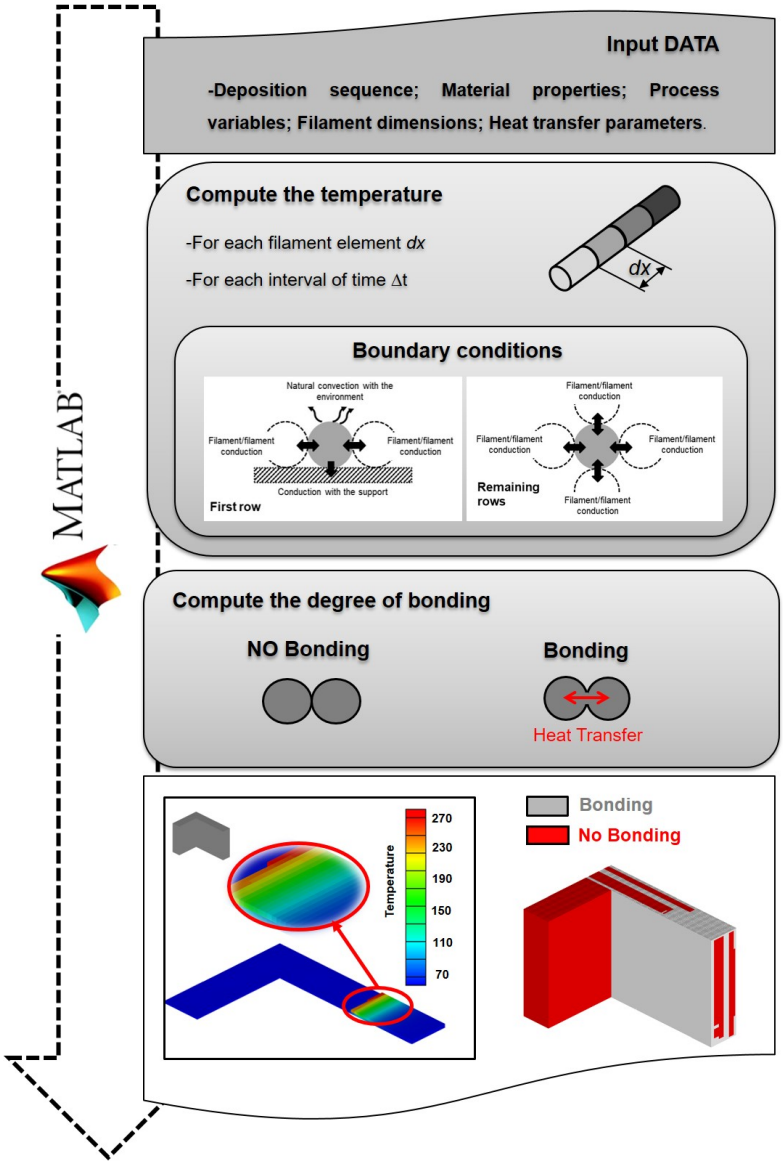

Fig. 7 Simplified flowchart of the computer code.

The predictions were experimentally validated [13]. For example, Figure 8 concerns the deposition of a vertical stack of 3 filaments. The plots are made for a

vertical cross-section distant 40 mm from the edge. Under the processing conditions used, the top filament was laid 6.7 s after the one in the middle, and 17.6 s after that at the bottom. The measured temperatures are in excellent agreement with the predictions.

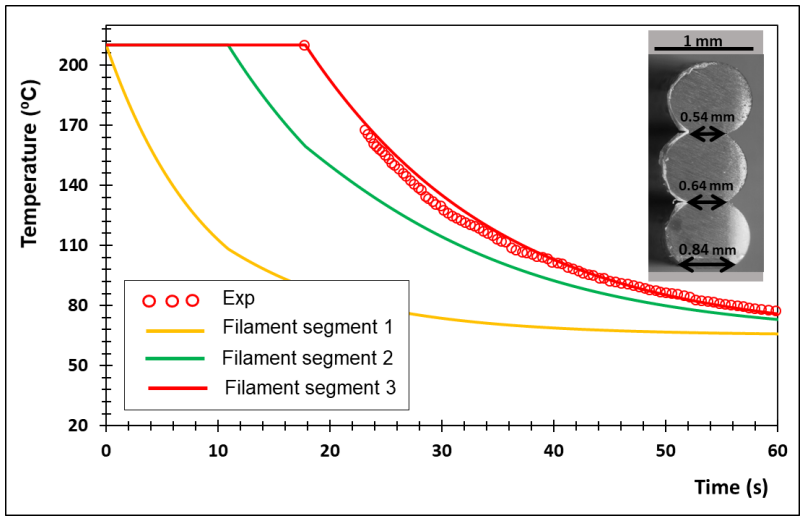

Fig. 8 Temperature evolution with time (at a vertical cross-section distant 40 mm from the edge) of a vertical stack of 3 filament segments (die set to 220ºC) (adapted from [13]).

Figures 9 and 10 illustrate the modelling capabilities of the code. Figure 9 depicts the time evolution of the temperature of ABS filaments 1–9 at a vertical cross-section at mid-length of the structure schematized in the inset. When a new filament is deposited, the temperature of the contacting filaments (previously deposited) increases and so their cooling is delayed. Even filament 1, which was the first to be deposited, is affected by the depostion of the remaining 8 filaments, although only filament 2 is in contact with it. These physical contacts can alter the local filament temperatures by as much as 18ºC. This raise in temperature, together with the time period during which it occurs, might be useful for bonding. Figure 10 presents the predicted time that is required for bonding between all pairs of contacting filaments of the structure represented in the inset, for three different extrusion temperatures. As expected, the higher the extrusion temperature, the lower the time required for bonding. In general, the latter is quite short, typically less than 0.25s, but while at the highest extrusion temperature all contacting filament pairs achieve bonding, this is not the case for the other two temperatures. For example, at 230ºC there is no bonding between filaments 1&2 (the first two filaments to be deposited), bonding between 2&3 and no bonding for pair 3&4. If there is no bonding, heat transfer

between filamentss 1 and 2 is limited. As a consequence, filament 2 remains sufficiently hot to bond to filament 3 when contact arises. For the same reasons, filament 3 cools faster and will not be able to bond to filament 4.

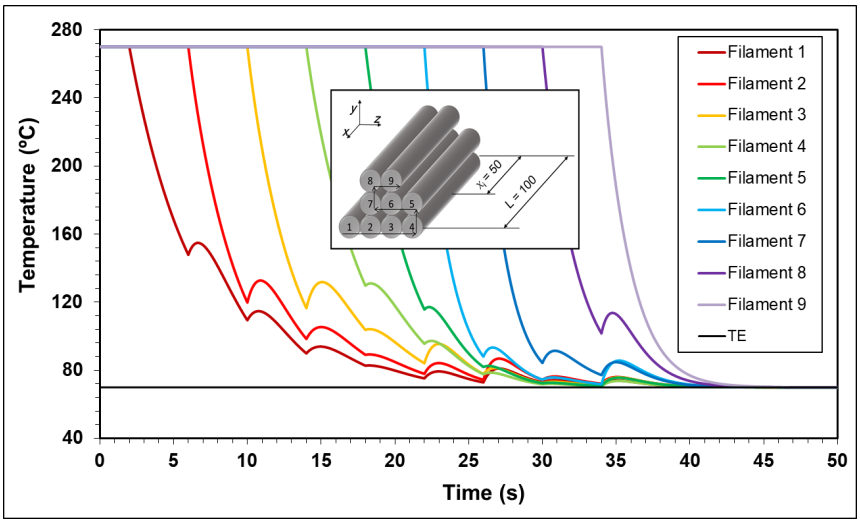

Fig. 9 Temperature evolution with time of filaments 1–9 for the geometry and deposition sequence illustrated in the inset at a vertical cross-section distant 50 mm from the edge (adapted from [13])

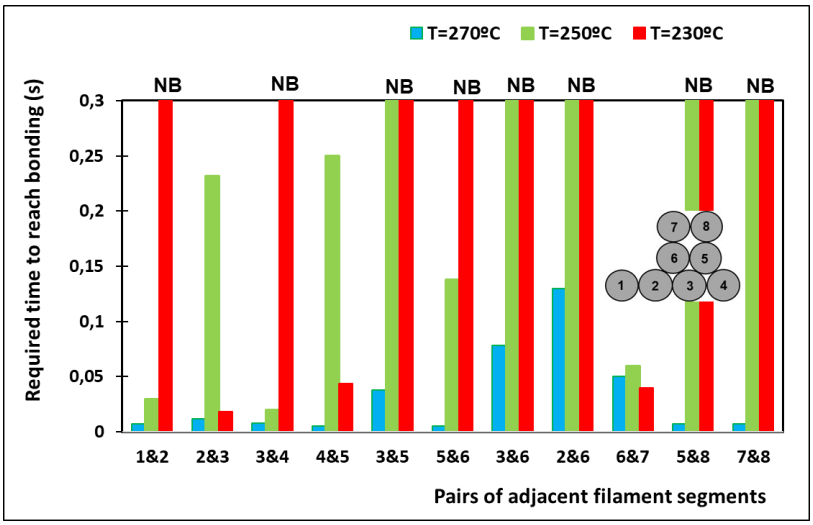

Fig. 10 Time required to achieve bonding between pairs of adjacent filaments segments for the geometry illustrated in the inset, at a vertical cross-section distant 50mm from the edge. NB –No Bonding (adapted from [13])

3. Effect of processing parameters on bonding

The part shown in Figure 11 will be considered in order to study the effect of processing parameters on the quality of bonding. It can be manufactured using six different build orientations (denoted as A do F), as demonstrated in Figure 12.

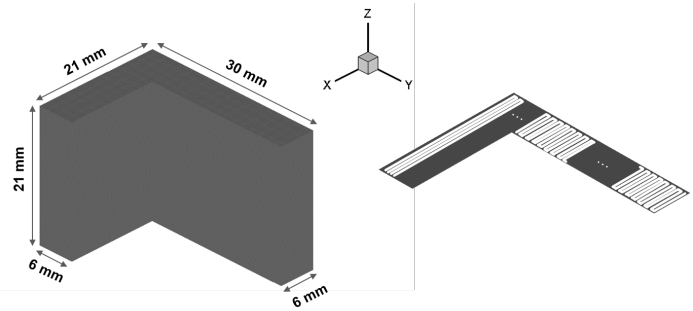

Fig. 11 Geometry, dimensions and deposition sequence (unidirectional aligned with 100% fill) of the part studied

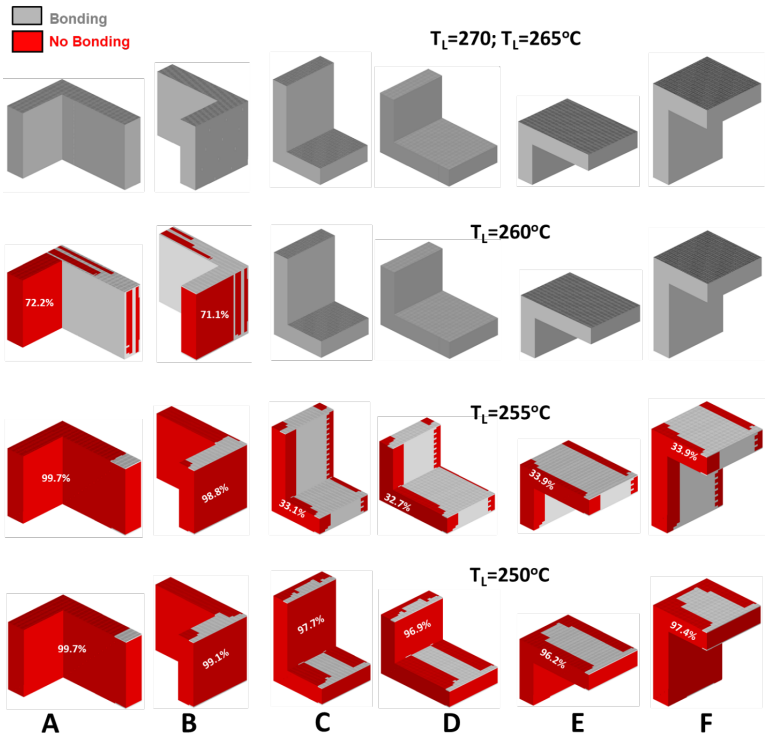

Fig.12 Influence of build orientation and extrusion temperature on bonding (environment temperature of 70°C).

Orientations labelled E and F require support material. Orientations A to D involve the deposition of 3000 filaments, while orientations E and F are built from 7000 filaments. Obviously, this will result in different manufacturing times. Figure 12 gathers predictions of bonding quality (in terms of volume fraction of the part with bonding being achieved between filaments) when printing with different extrusion temperatures and using the six build orientations. For extrusion temperatures of 265ºC or 270ºC (typical extrusion temperature for ABS, a common polymer used in FFF), all parts exhibit good quality. When this temperature decreases, quality deteriorates progressively, and some delamination may become likely. At 250ºC, the parts should have little mechanical resistance. At constant extrusion temperature, build orientations A and B yield the worst bonding quality, while the remaining seem equivalent. However, orientations E and F entail longer manufacturing times.

Figure 13 represents graphically the correlation between extrusion temperature and bonding, for the various build conditions. Orientations A and B require extrusion temperatures 5ºC – 8ºC higher than the remaining to achieve parts with similar quality. The data follows two distinct patterns, one for orientations A and B, another for orientations C to F.

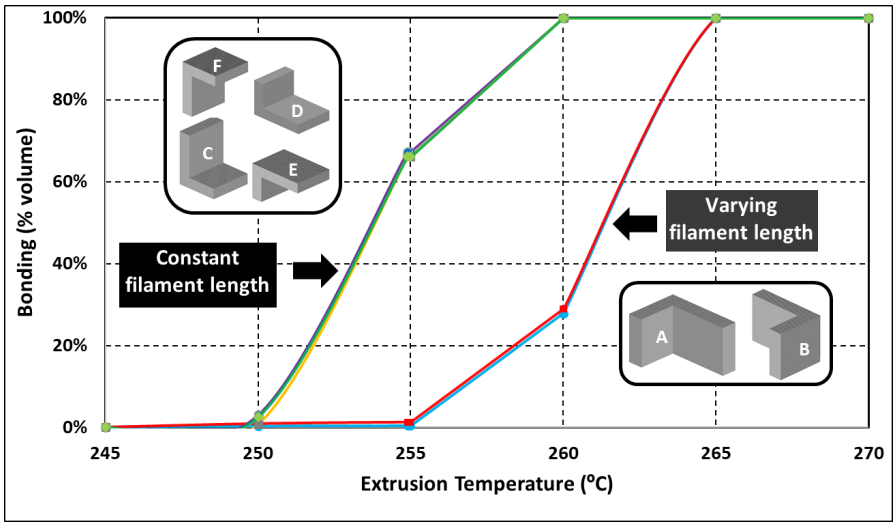

Fig. 13 Correlation between extrusion temperature and bonding, for various build conditions

As observed in Figure 11 (and indicated in Figure 13) build orientation A entails the deposition of long filaments in one side of the part, followed by short filaments in the another side. The reverse occurs for build orientation B.

However, in the remaining build orientations, the filaments have equal length. Since the printing velocity is constant, contacts between longer filaments occur at higher time intervals. Thus, these filaments are likely to cool down significantly before re-heating due to contact with a newly deposited filament. Simultaneously, the temperature raise may not be sufficient for bonding. This is further illustrated in Figure 14, which shows four snapshots of temperature at 10, 30, 45 and 75s of the deposition sequence for build orientation A, when extruding at 260ºC.

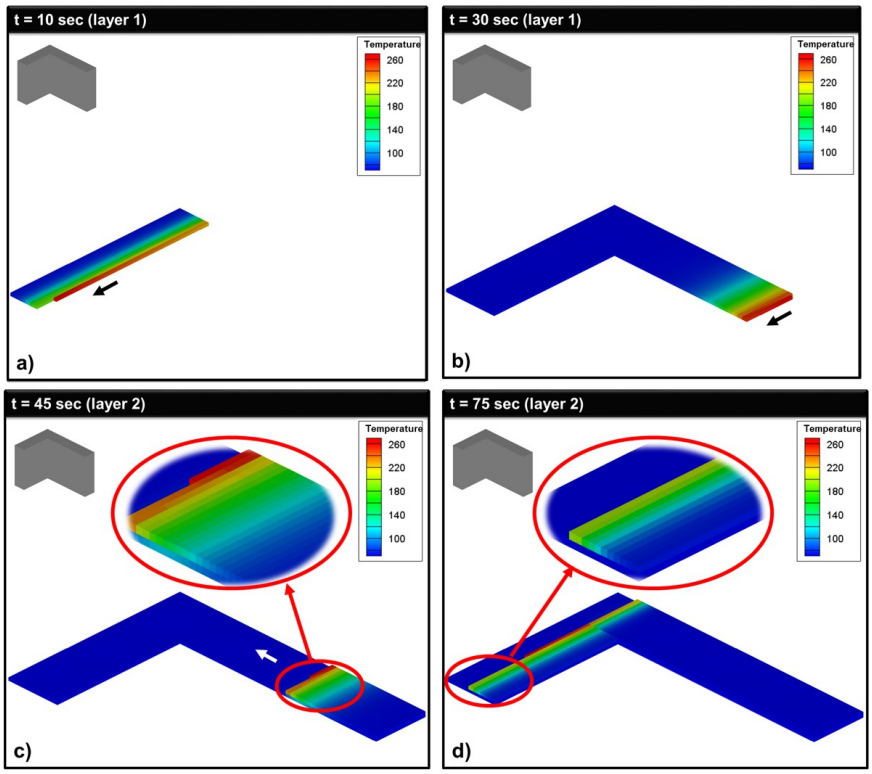

Fig. 14 Snapshots of material temperature at various instants of printing (build orientation A, extrusion temperature of 260ºC)

Printing begins at the left side of the first layer, which requires long filaments (Figure 14a). Then, the right side of the same layer is printed using short filaments (Figure 14b). The second layer is then laid, starting from the right side and progressively moving towards the left. This means that the new filaments of the second layer will be able to sufficiently re-heat the colder segments underneath to a temperature (during sufficient time) enabling bonding (Figure 14c). However, when printing the left hand side (figure 14d) the new filaments will be unable to reheat

meaningfully those of the first layer, as a long time since deposition of the latter has elapsed.

Close observation of the bonding quality shown in Figure 12 reveals regions alternating between bonding and no bonding, especially at 260ºC and for build orientations A and B. As discussed above and drafted in Figure 15 (left), if two filaments (1 and 2) become in contact after a long time, bonding will not be achieved. Filament 2 will remain relatively hot. Thus, when filament 3 contacts filament 2, bonding will be likely, if the time involved is sufficiently low. This sequence will continue, i.e., when filament 4 contacts filament 3, the time elapsed for their contact will determine whether bonding will occur. In more general terms, the lack of bonding between a pair of filaments prevents efficient heat transfer between them, causing slower cooling. In turn, might facilitate bonding with a newer hot filament. Conversely, when bonding develops, the higher heat transfer between them will promote faster cooling, which can hinder bonding with a newer filament (see illustration in Fig.15 (right)). The process is governed by the geometry of the part, build orientation and deposition sequence, but can be influenced by a proper choice of processing temperatures.

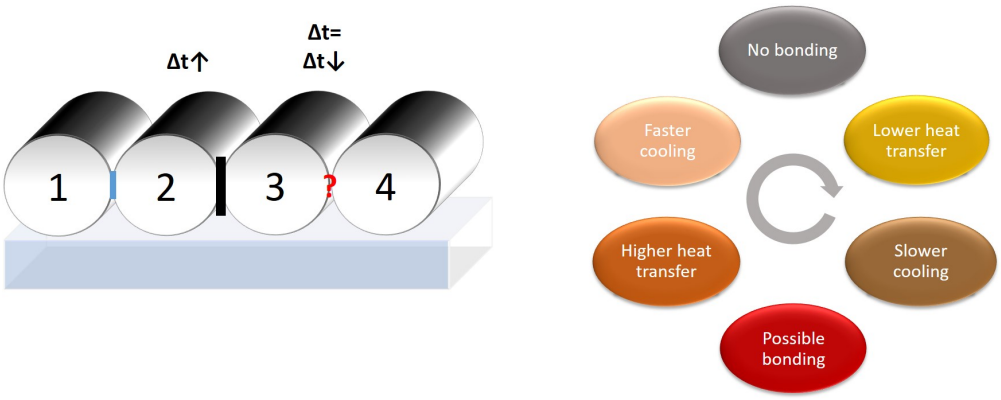

Fig. 15 A schematic explanation of how bonding between two filaments can hinder bonding with a third, newer filament

4. Selecting the printing conditions of a practical part

FFF are particulary advantageous for the manufacture of surgical instruments, due to their flexibility in terms of part geometry, easy adaptation to specific needs, and rapid manufacture. Figure 16 presents a scalpel handle, to be manufactured in ABS. Adopting unidirectional and aligned filament deposition and typical processing

conditions for ABS, it will take approximately 12 minutes to print the handle. Due to the geometry and thickness of the part, only two build orientations are feasible (Figure 16). They involve filament lengths ranging between 78 and 110 mm (orientation 1) and between 3 and 15 mm (orientation 2), respectively, thus affecting the instants at which contacts arise during deposition.

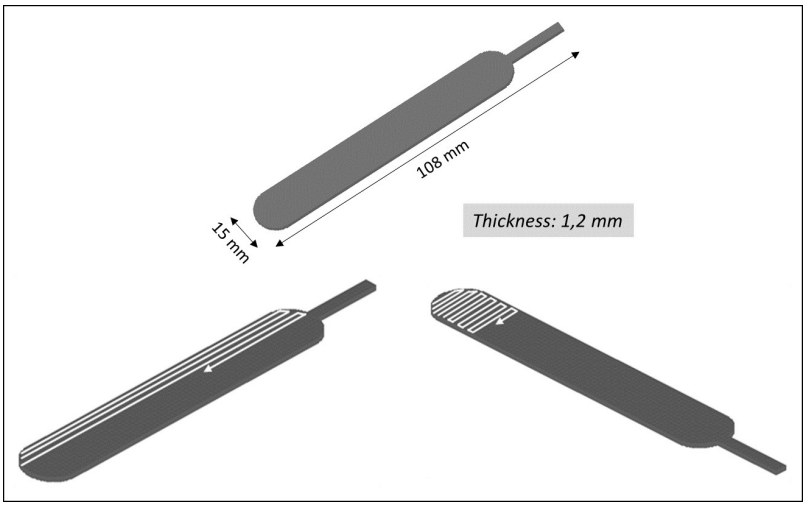

Fig. 16 Scalpel handle. Geometry of the part (top); build orientations (bottom)(left: orientation 1, involving 4 layers and 200 filaments; right: orientation 2, involving 4 layers and 1440 filaments).

Figure 17 predicts the correlation between extrusion temperature (ranging from 245 to 270ºC) and bonding, for the two build orientations. Below 260ºC, the handles will show poor mechanical performance. Raising the extrusion temperature to 270ºC solves the problem, which corroborates the practical choice of this temperature by most commercial 3D printers. Still, good parts could be obtained already at 265ºC, with build orientation 2. These predictions were made considering that the 3D printer is fitted with a (forced) convection oven with controlled temperature, which was kept at 70ºC. However, the most popular equipment operates at room temperature. Thus, assuming build orientation 2, natural convection, and the environment and support temperature $T_E = T_{sup} = 25$ºC, Figure 18 presents bonding predictions for extrusion temperatures of 270ºC and 300ºC. Even raising the extrusion temperature well beyond its usual value, a handle with poor quality will be always obtained. As expected, bonding will be achieved only in the narrower edge, since here filaments are shorter and contact each other more frequently.

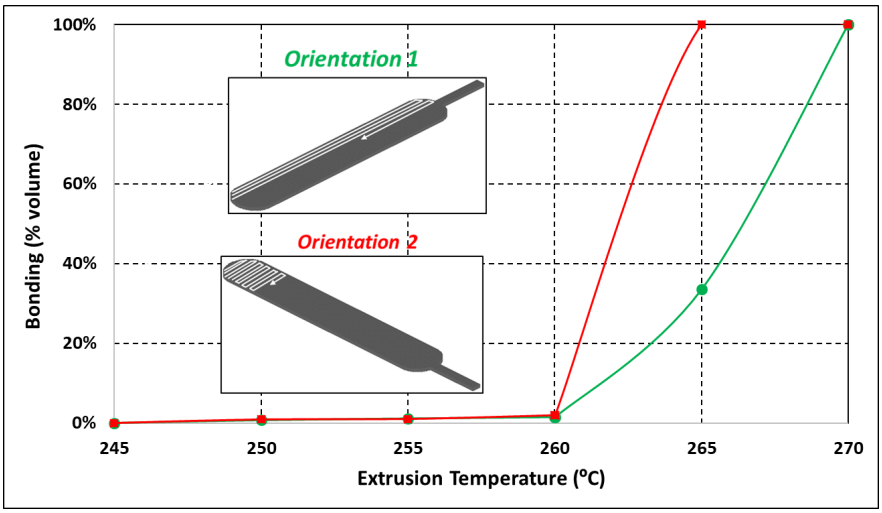

Fig. 17 Correlation between extrusion temperature and bonding of the scalpel handle, for two build conditions.

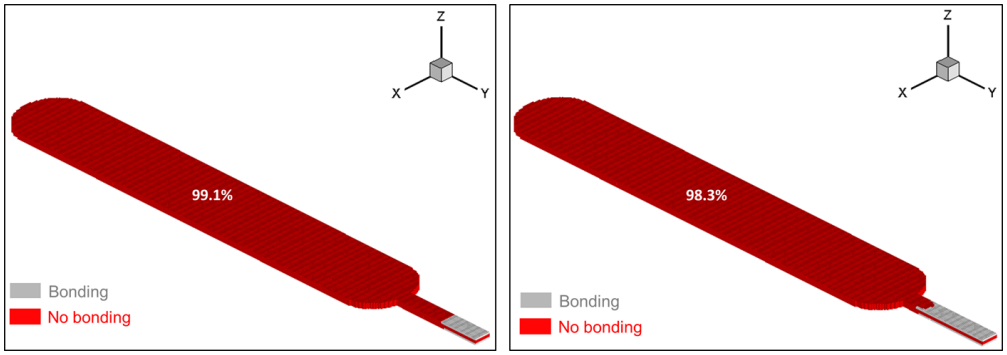

Fig. 18 Bonding predictions for build orientation 2, natural convection, environment and support temperature of 25ºC, extrusion velocity of 0.025m/s, for extrusion temperatures of 270ºC (left) and 300ºC (right).

One possible processing strategy to balance the heat losses to the environment would be to increase the extrusion velocity, as this would reduce the time between contacts. As seen in Figure 19, this route was only partially successful. When duplicating the extrusion velocity from 0.025m/s to 0.05m/s, the percentage of the part with poor bonding remained very high, albeit decreasing to 68% if extrusion is performed at 300ºC.

In practice, most 3D printers allow to heat the support. Figure 20 displays bonding predictions assuming that the support is kept at T_{sup} = 100ºC, for two values of the thermal contact conductance with the support, extrusion velocity of 0.025m/s, and extrusion temperature of 270ºC. If the thermal conductance is sufficiently high, it is possible to obtain approximately half of the part with good bonding.

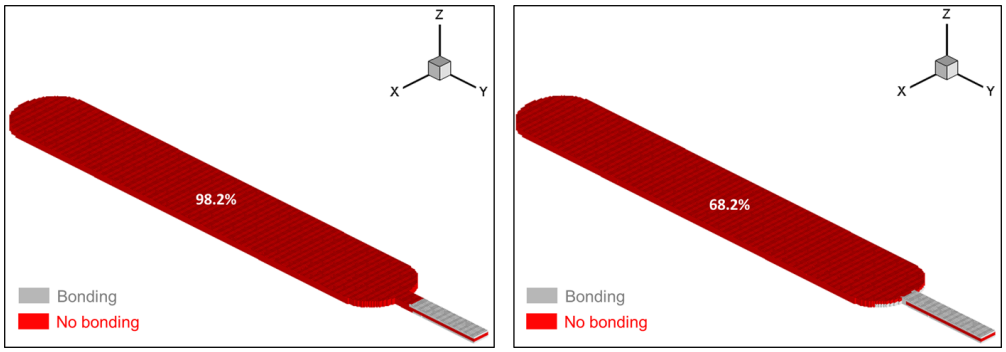

Fig. 19 Bonding predictions for build orientation 2, natural convection, environment and support temperature of 25ºC, extrusion velocity of 0.05m/s, for extrusion temperatures of 270ºC (left) and 300ºC (right).

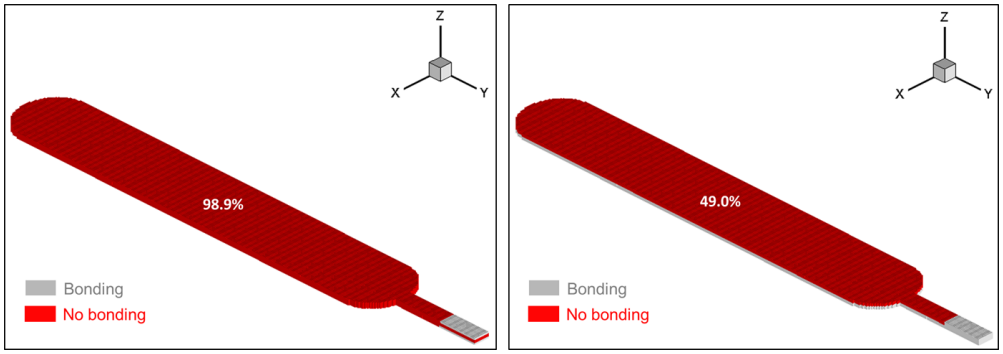

Fig. 20 Bonding predictions for build orientation 2, extrusion temperature of 270ºC, natural convection, environment temperature of 25ºC, support temperature of 100ºC, extrusion velocity of 0.025m/s, for thermal conductances of h_{sup}=10W/m^2.ºC (left) and h_{sup}=150W/m^2.ºC. (right).

5. Conclusions

This chapter studied FFF from a phenomenological point of view, focusing on the deposition and cooling stage due to its relevance to the characteristics of the final printed parts. Heat transfer is complex, and strongly influenced by both the geometry of the part and processing conditions. Therefore, process modelling tools can be quite useful not only to better understand the prevailing heat transfer mechanisms and related influencing parameters, but also to support the definition of adequate operating conditions for practical parts. The results showed that, whenever possible, 3D printers should be fitted with a convection oven, due to its helpful effect on bonding, which cannot be fully balanced by tuning other process parameters.

References

[1] J. R. C. Dizona, A. H. Espera Jr., Q. Chena, R. C. Advincula, Mechanical characterization of 3D-printed polymers. Addit. Manuf. 20 (2018) 44–67.

[2] S. Hertle, M. Drexler, D. Drummer, Additive Manufacturing of Poly(propylene) by Means of Melt Extrusion. Macromol. Mater. Eng. 301 (2016), 1482–1493.

[3] J. Gonçalves, P. Lima, B. Krause, P. Poetschke, U. Lafont, J. Gomes, C. Abreu, M. C. Paiva, J. A. Covas, Electrically conductive Polyetheretherketone nanocomposite filaments: from production to Fused Deposition Modelling, Polymers 10 (2018), 925-945

[4] A. Kantaros and D. Karalekas, Fiber Bragg grating based investigation of residual strains in ABS parts fabricated by fused deposition modelling process. Mater. Des. 50 (2013) 44–50.

[5] B. Céline, L. Longmei, Q. Sun, Q., P. Gu. Modelling of bond formation between polymer filaments in the fused deposition modelling process. J. Manuf. Process. 6 (2004) 170–178.

[6] Q. Sun, G. M. Rizvi, C. T. Bellehumeur, P. Gu, Effect of processing conditions on the bonding quality of FDM. Rapid Prototyp. J., 14 (2008) 72–80.

[7]] P.K. Gurrala, S. P. Regalla, Part strength evolution with bonding between filaments in fused deposition modelling. Virtual Phys. Prototyp. 9 (2014) 141–149.

[8]] M. A. Yardimci and S. Güçeri, Conceptual framework for the thermal process modelling of fused deposition, Rapid Prototyp. J., 2 (1996) 26-31.

[9] M. A. Yardimci, S. Güçeri., S. C. Danforth, 1997. Thermal analysis offused deposition. In: Proceedings in Solid Freeform Fabrication Symposium,Austin, TX (1997) 689–698.

[10] J. F. Rodriguez, J. P. Thomas, J. E. Renaud, J.E., 2000. Characterization of themesostructure of fused-deposition acrylonitrile-butadiene-styrene materials. Rapid Prototyp. J. 6, 175–185.

[11] J. F. Rodriguez, J. P. Thomas, J. E. Renaud, Design of fused-deposition ABScomponents for stiffness and strength. J. Mech. Des. 125 (2003) 545–551.

[12] - A. D'Amico, A. M. Peterson, An adaptable FEA simulation of material extrusion additive manufacturing heat transfer in 3D, Addit. Manuf. 21 (2018), 422–430.

[13] S. F. Costa, F. M Duarte, J. A. Covas, Estimation of filament temperature and adhesion development in Fused Deposition Techniques, J. Mat. Proc. Techn., 245 (2017) 167–179.
[14] Y. Zhang and V. Shapiro V. Linear-Time Thermal Simulation of As-Manufactured Fused Deposition Modeling Components, Journal of Manufacturing Science and Engineering, 140 (2018) 1-11.
[15] S. F. Costa, F. M. Duarte, J. A. Covas, Thermal conditions affecting heat transfer in FDM/FFE: a contribution towards the numerical modelling of the process, Virtual Phys. Prototyp., 10 (2015) 35-46
[16] J. Mueller and K. Shea, Buckling, build orientation, and scaling effects in 3D printed lattices, Mats. Today Commun., 17 (2018) 69-75
[17] P. K. Wah, K. G. Murty, A. Joneja, L. C. Chiu, Tool path optimi-zation in layered manufacturing. IEEE Transactions 34 (2002) 335–3479.
[18] G. Dreifus, K. Goodrick, S. Giles, M. Patel, R. M. Foster, C. Williams, J. Lindahl, B. Post, A. Roschli, L. Love, V. Kunc, Path optimization along lattices in additive manufacturing using the Chinesepostman problem. 3D. Print Addit Manuf 4 (2017) 98–10).
[19] N. Volpato and T. T. Zanotto, Analysis of deposition sequence in tool-path optimization for low-costmaterial extrusion additive manufacturing, The International Journal of Advanced Manufacturing Technology 101v(2019)v1855–1863.
[20] F. Yang and R. Pitchumani, Healing of Thermoplastic Polymers at an interface under Nonisothermal Conditions, Macromolecules, 35 (2002) 3213-3224.